Quantum dynamics of localized excitations in a symmetric trimer molecule

R. A. Pinto and S. Flach

Max-Planck-Institut für Physik komplexer Systeme, Nöthnitzer Strasse 38, 01187 Dresden, Germany
(Received 26 July 2005; published 24 February 2006)

We study the time evolution of localized (local bond) excitations in a symmetric quantum trimer molecule. We relate the dynamical properties of localized excitations such as their spectral intensity and their temporal evolution (survival probability and tunneling of bosons) to their degree of overlap with quantum tunneling pair states. We report on the existence of degeneracy points in the trimer eigenvalue spectrum for specific values of parameters due to avoided crossings between tunneling pair states and additional states. The tunneling of localized excitations which overlap with these degenerate states is suppressed at all times. As a result local bond excitations may be strongly localized forever, similar to their classical counterparts.

I. INTRODUCTION

The study of the classical and quantum dynamics of excitations in nonlinear systems with few degrees of freedom has been used for decades to understand the processes of energy redistribution after an initial local bond excitation in polyatomic molecules [1–6]. Equally, interest in these issues evolved from the more mathematical perspective of nonlinear dynamics, localization of energy, and solitons [7]. This second path was boosted by the observation of discrete breathers (DBs)—time-periodic and spatially localized excitations—in a huge variety of spatially discrete lattice systems [8–11]. The flood of recent experimental observations of DBs in various systems includes such different systems as bond excitations in molecules, lattice vibrations and spin excitations in solids, electronic currents in coupled Josephson junctions, light propagation in interacting optical waveguides, cantilever vibrations in micromechanical arrays, cold atom dynamics in Bose-Einstein condensates loaded on optical lattices, among others [12–22]. In a substantial part of these cases quantum dynamics of excitations is either unavoidable (molecules, solids) or reachable by corresponding parameter tuning (Josephson junctions, Bose-Einstein condensates).

Progress in classical theory was achieved using a synergy of analytical results and computational approaches. The computational aspect is vital because we deal generically with nonintegrable systems, which cannot be completely solved analytically. Computational studies of classical systems of many interacting degrees of freedom (say N oscillators) are straightforward since we have to integrate $2N$ coupled first-order ordinary differential equations, so $N \sim 10^4$ is no obstacle to doing even long-time simulations in order to study statistical properties. The quantum case is much less accessible by computational studies. This is because in general each degree of freedom (e.g., an oscillator) is now embedded in an infinite-dimensional Hilbert space. Even after restricting to only s states per oscillator, the dimension of the Hilbert space of the interacting system is now s^N, making it nearly impossible to treat both large values of s and N—independent of whether we aim at integrating the time-dependent Schrödinger equation or diagonalizing the corresponding Hamiltonian. However, it is possible to treat small

systems with $N=2,3$, which adds to the above-mentioned studies of bond excitations in molecules, prospective cases of few coupled Josephson junctions, and Bose-Einstein condensates in optical traps with just a few wells [23,24]. Remarkably, in the last case there is already an experimental realization [25].

Extensive studies of a dimer model $N=2$ with additional conservation of the number of excitations (bosons) have been accomplished [26–33]. The conservation of energy and boson number makes this system integrable. Due to the nonlinearity of the model the invariance under permutation of the two sites (bonds, spin flips, etc.) does not prevent it from having classical trajectories which are not invariant under permutations. These trajectories correspond to a majority of bosons (and thus energy) being concentrated on one of the sites. Quantum mechanics reinforces the symmetry of the eigenstates via dynamical tunneling in phase space (without obvious potential energy barriers being present) [34]. The tunneling time is inversely proportional to the energy splitting of the corresponding tunneling pairs of eigenstates. Notice that while most of the quantum computations concerned diagonalization of the Hamiltonian, a few results show consistency with numerical integration of the Schrödinger equation [31,36]. In [25] experimental observation of nonlinearity-induced localization of Bose-Einstein condensates in a double-well system was obtained, in agreement with results discussed above.

The extension of the dimer to a trimer $N=3$ allows one to study the fate of the tunneling pairs in the presence of nonintegrability [35–40] and in the effective presence of fluctuation of the number of bosons (on the dimer). Diagonalization showed that tunneling pairs survive up to a critical strength of nonintegrability [36], while the pair splittings showed characteristic resonances due to interactions with other eigenstates [40].

Trimer models have been also extensively studied in order to describe spectral properties and thus energy transfer in *ABA* molecules like water [41–45], which is connected with the appearance of quantum local modes (discrete breathers). In these studies the presence of local modes was already identified as nearly degenerate eigenstates (tunneling pairs) in the eigenvalue spectra of the considered systems.

In this work we study the time evolution of localized excitations in the trimer, and compare with the spectral properties of the system. We compute the eigenvalues and eigenstates of the quantum system and then the expectation values of the number of bosons at every site on the trimer and the survival probability of different initial excitations as a function of time. We also compute the spectral intensity of the initial excitations to see how many eigenstates are overlapping. That allows one to draw conclusions about the correspondence between the time evolution of a localized initial quantum state (not an eigenstate) and the presence or absence of quantum breathers, i.e., dynamical tunneling eigenstates. We identify degeneracies in the trimer spectrum due to avoided crossings, and relate these events to unusual classical-like behaviour of quantum localized excitations.

II. LOCAL BOND EXCITATIONS IN THE CLASSICAL CASE

The classical trimer is described by the Hamiltonian [36]

$$H = H_d + \frac{1}{2}(P_3^2 + X_3^2) + \frac{\delta}{2}(X_1X_3 + P_1P_3 + X_2X_3 + P_2P_3),$$

(1)

$$H_d = \frac{1}{2}(P_1^2 + P_2^2 + X_1^2 + X_2^2) + \frac{1}{8}[(P_1^2 + X_1^2)^2 + (P_2^2 + X_2^2)^2]$$

$$+ \frac{C}{2}(X_1X_2 + P_1P_2),$$

(2)

where H_d is the dimer part. In all of this work we use dimensionless quantities. C is the coupling inside the dimer, and δ is the coupling between site 3 and the dimer, which also destroys the integrability of the system. Using the transformation $\Psi_i = (1/\sqrt{2})(X_i + iP_i)$ the Hamiltonian becomes

$$H = H_d + \Psi_3^*\Psi_3 + \delta(\Psi_1^*\Psi_3 + \Psi_2^*\Psi_3 + \text{c.c.}),$$

(3)

$$H_d = \Psi_1^*\Psi_1 + \Psi_2^*\Psi_2 + \frac{1}{2}[(\Psi_1^*\Psi_1)^2 + (\Psi_2^*\Psi_2)^2] + C(\Psi_1^*\Psi_2$$

$$+ \text{c.c.}),$$

(4)

and the equations of motion transform to $i\dot{\Psi}_i = \partial H/\partial \Psi_i^*$. Note that the total norm $B = \Psi_1^*\Psi_1 + \Psi_2^*\Psi_2 + \Psi_3^*\Psi_3$ is conserved, and hence the problem is effectively two dimensional. Also the trimer (and the dimer) is invariant under permutation of sites 1 and 2.

We are interested in the fate of localized excitations, where some energy is excited, e.g., on site 1, and none on site 2 (inside the dimer). The third site may have some nonzero energy as well (like an environment). For different initial conditions

$$\Psi_1(0) = \sqrt{\frac{B}{2} + \nu}, \quad \Psi_2(0) = 0, \quad \Psi_3(0) = \sqrt{\frac{B}{2} - \nu}, \quad (5)$$

we computed the time evolution of the quantities $|\Psi_i|^2 = \Psi_i^*\Psi_i$ by numerically solving the equations of motion. In
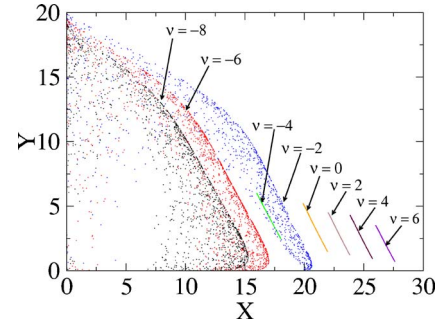
all computations we used $B = 40$, $C = 2$, and $\delta = 1$. We also generate a Poincaré map (Fig. 1) using the condition $\Delta_{13} = 0$ $(\Psi_i = A_i e^{i\varphi_i}, \Delta_{ij} = \varphi_i - \varphi_j)$ and the plane $X = |\Psi_1|^2$, $Y = |\Psi_2|^2$. We observe that for positive ν the evolution is regular and not invariant under permutation, so most of the energy initially placed on site 1 stays there, with site 2 becoming only little excited. Negative values of ν yield chaotic motion which is permutation invariant.

This transition from localization to delocalization of energy is also nicely observed in the temporal evolution in Fig. 2. Increasing ν from negative to positive values, the energy exchange between sites 1 and 2 of the dimer is stopped.

III. LOCAL BOND EXCITATIONS IN THE QUANTUM TRIMER

The quantum trimer is obtained after replacing the complex functions Ψ, Ψ^* by the bosonic operators a and $a^\dagger$ [rewriting $\Psi^*\Psi = (1/2)(\Psi^*\Psi + \Psi\Psi^*)$ previously to ensure the invariance under exchange $\Psi \leftrightarrow \Psi^*$]:
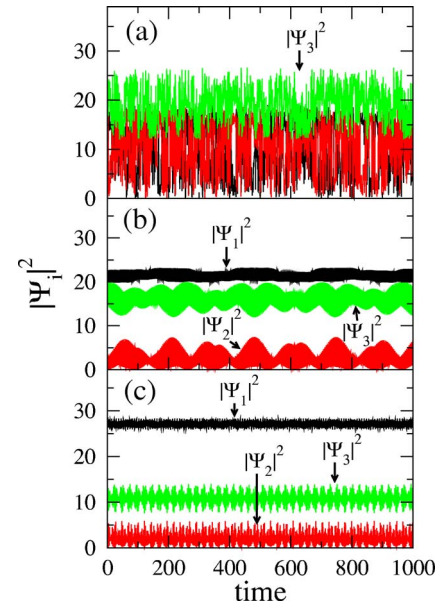

FIG. 1. (Color online) Poincaré map of the classical phase-space flow of the trimer. The map condition is $\Delta_{13} = 0$. The plotting plane is $X = |\Psi_1|^2$ and $Y = |\Psi_2|^2$. The parameters are $B = 40$, $C = 2$, $\delta = 1$.

FIG. 2. (Color online) Time evolution of $|\Psi_i|^2$ ($i = 1, 2, 3$) for different initial states $\Psi_{1,3}(0) = \sqrt{20 \pm \nu}$ [$\Psi_2(0) = 0$]: $\nu =$ (a) -6, (b) 0, and (c) 6.

$$\hat{H} = \hat{H}_d + \frac{3}{2}\hat{a}_3^\dagger\hat{a}_3 + \delta(\hat{a}_1^\dagger\hat{a}_3 + \hat{a}_2^\dagger\hat{a}_3 + \text{c.c.}), \qquad (6)$$

$$\hat{H}_d = \frac{15}{8} + \frac{3}{2}(\hat{a}_1^\dagger\hat{a}_1 + \hat{a}_2^\dagger\hat{a}_2) + \frac{1}{2}[(\hat{a}_1^\dagger\hat{a}_1)^2 + (\hat{a}_2^\dagger\hat{a}_2)^2]$$
$$+ C(\hat{a}_1^\dagger\hat{a}_2 + \text{c.c.}), \qquad (7)$$

where we take $\hbar = 1$. The boson number operator $\hat{B} = \hat{a}_1^\dagger\hat{a}_1 + \hat{a}_2^\dagger\hat{a}_2 + \hat{a}_3^\dagger\hat{a}_3$ commutes with the Hamiltonian, so we may diagonalize (6) in the basis of eigenfunctions of $\hat{B}$, $\{|n_1, n_2, n_3\rangle\}$, where $n_1, n_2,$ and n_3, respectively, are the numbers of bosons at sites 1, 2, and 3. There are $(b+1)(b+2)/2$ eigenstates in the subspace corresponding to a fixed value of the eigenvalue b of $\hat{B}$. Since the Hamiltonian is invariant under permutation between sites 1 and 2 we expanded the wave function in the basis of symmetric and antisymmetric eigenstates of $\hat{B}$, $\{|n_1, n_2, n_3\rangle_{S,A}\}$, where

$$|n_1, n_2, n_3\rangle_{S,A} = \frac{1}{\sqrt{2}}(|n_1, n_2, n_3\rangle \pm |n_2, n_1, n_3\rangle). \qquad (8)$$

Then the initial state $|\Psi_0\rangle = |n_0, m_0, l_0\rangle$ is written as

$$|\Psi_0\rangle = \frac{1}{\sqrt{2}}(|n_0, m_0, l_0\rangle_S + |n_0, m_0, l_0\rangle_A), \equiv \frac{1}{\sqrt{2}}(|\Psi_0\rangle_S + |\Psi_0\rangle_A). \qquad (9)$$

In this representation diagonalization of the Hamiltonian reduces to diagonalizing two smaller matrices—symmetric and antisymmetric decompositions of $\hat{H}$—whose eigenvalues are $E_\mu^{(S,A)}$, with less computing cost than diagonalization of the full Hamiltonian. All computations were done using this representation.

We computed the time evolution of expectation values of the number of bosons at every site on the trimer $\langle n_i \rangle(t) = \langle \Psi_t | \hat{n}_i | \Psi_t \rangle$ and the survival probability $P_t = |\langle \Psi_0 | \Psi_t \rangle|^2$ (see the Appendix for explicit expressions), starting with various boson number distributions among sites 1 and 3 controlled by the number ν: $|\Psi_0\rangle = |b/2 + \nu, 0, b/2 - \nu\rangle$, with $b = 40$, $C = 2$, and $\delta = 1$. In computations we dropped the two first terms of the Hamiltonian, which are diagonal and just shift the spectrum.

A. Tunneling pairs and localization

In Fig. 3 we show the time evolution of expectation values of the number of bosons in the trimer. When the initial excitation is mainly localized at the third site in the trimer there is a fast redistribution of bosons between the two sites in the nonlinear dimer until the dimer sites are equally occupied [Fig. 3(a)]. As we place more bosons on the dimer (site 1) the tunneling time of the excitation increases rapidly until the time of computation becomes too short to observe slow tunneling. On these time scales we thus observe localization of bosons on one site in the dimer [Figs. 3(b) and 3(c)], in analogy to the classical case. The reason for this behavior is the appearance of *tunneling pairs* of symmetric and antisym-
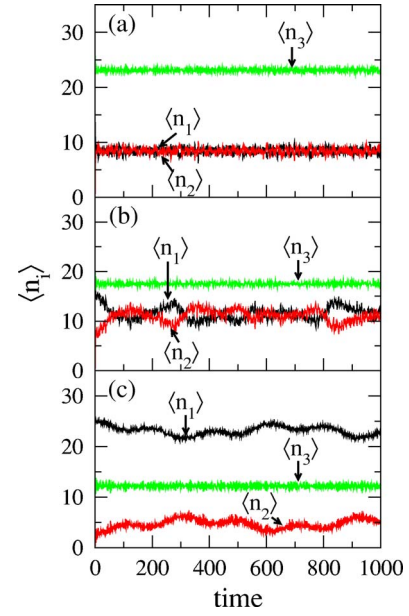

FIG. 3. (Color online) Time evolution of expectation values of the number of bosons at each site of the trimer for different initial states $|\Psi_0\rangle = |20 + \nu, 0, 20 - \nu\rangle$: $\nu =$ (a) -6, (b) 0, and (c) 6.

metric eigenstates with very close eigenenergies in comparison to the mean energy separation between eigenstates (Fig. 5 below). These pairs strongly overlap with the initial state, as observable from the spectral intensity $I_\mu^0 = |\phi_\mu^0|^2$ in the inset of the Fig. 4.

The results in Fig. 4 show an enhancement of the survival probability with increasing boson number at site 1, which is consistent with the results discussed above. The dominant tunneling pairs in the spectral intensity (inset of Fig. 4) give
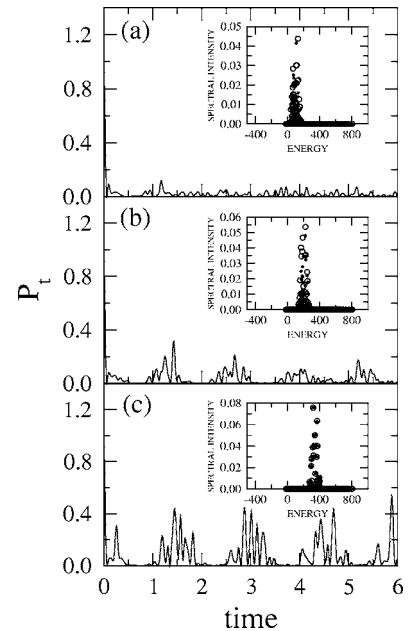

FIG. 4. Survival probability of the initial state $|\Psi_0\rangle = |20 + \nu, 0, 20 - \nu\rangle$. $\nu =$ (a) -6, (b) 0, and (c) 6. Inset: Spectral intensity of the initial state $|\Psi_0\rangle$. Filled circles, symmetric eigenstates; open circles, antisymmetric eigenstates.
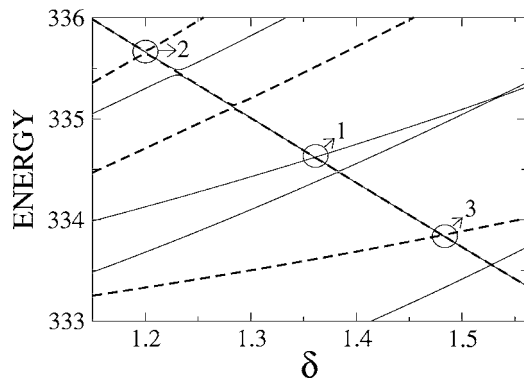
FIG. 5. An enlargement of the trimer spectrum showing three particular pair–single-state interactions (numbered circles). Thin solid line, symmetric eigenstates; thick dashed lines, antisymmetric eigenstates.
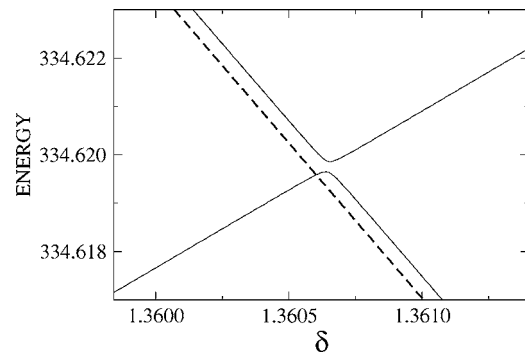

FIG. 6. An enlargement of the trimer spectrum around the avoided crossing 1 in Fig. 5, involving the antisymmetric state A-268 (thick dashed line) and the symmetric states S-286 and S-285 (thin solid lines).

the main contribution to the time dependence of the survival probability [36].

B. Avoided crossings and degenerate eigenstates

Energy levels exhibit avoided crossings when we vary the parameter δ which regulates the strength of nonintegrability of the system [36], as shown in Fig. 5. Of particular interest is the outcome of the interaction of a single eigenstate and a tunneling pair. The principal difference between these states is that the member of a tunneling pair has exponentially small weight in the dynamical barrier region, which is roughly defined by $n_1 = n_2$ in the n_1-n_2 plane. A single eigenstate will in general have much larger weight in this region. Since each eigenstate is either symmetric or antisymmetric, and a tunneling pair consists always of states with both symmetries, the interaction with a third eigenstate will in general allow for an exact degeneracy of two states with different symmetries. While this is in principle possible for any two states of different symmetry, the exponentially small weight of the tunneling pair states in the dynamical barrier region makes a difference. Indeed, a linear combination of two states with large (not exponentially small) weight in a barrier region yields again an asymmetric state, but one with large weight in the barrier region. In contrast, for the case of a tunneling pair and a single state, we may expect an asymmetric eigenstate which has much less weight in the barrier region, leading to a much stronger localization of the state similar to a classical one.

We analyze three particular avoided crossings identified by numbered circles in Fig. 5 by computing the energy separation $\Delta E(\delta)$ between such a single state and a quantum breather tunneling pair. We identify three different situations. The first one shows that the energy levels intersect once at some degeneracy point (Fig. 6). At some value of the parameter δ the energy separation between one of the members of the tunneling pair and the single state vanishes. Tunneling is suppressed completely, and then an asymmetric linear combination of the degenerate eigenstates will constitute a non-decaying localized state. This situation has been well described by perturbation theory [40], where effects of other

eigenstates have been neglected. We computed the density $\rho(n_1, n_2) = |\langle n_1, n_2, n_3 | \phi \rangle|^2$ of the asymmetric eigenstate $|\phi\rangle = (|\phi_d^{(S)}\rangle + |\phi_d^{(A)}\rangle)/\sqrt{2}$, where $|\phi_d^{(S)}\rangle$ and $|\phi_d^{(A)}\rangle$ are the degenerate eigenstates. The result is shown in the Fig. 7 where we can see that there is only a partial localization of the excitation, since the wave function has visible contributions around the diagonal $X = Y$ ($n_1 = n_2$). Note that in addition it also shows a sizable contribution on the other side of the barrier ($n_1 \approx 2$, $n_2 \approx 26$ in Fig. 7). In fact the expectation values of the numbers of bosons for this state are $\langle n_1 \rangle = 14.99$, $\langle n_2 \rangle = 14.89$, $\langle n_3 \rangle = 10.12$. Thus in terms of averages practically no localization occurs since $\langle n_1 \rangle \approx \langle n_2 \rangle$ despite the observable asymmetry in Fig. 7.

The other two cases appear as a consequence of the influence of other states in the spectrum. In one case the energy levels do not intersect at all (Fig. 8), due to the presence of another avoided crossing located nearby. In the third case surprisingly we observe that the energy levels intersect twice. The situation is shown in Fig. 9, and is sketched in the inset of the figure. Due to the interaction with other states of the system we observe an intersection of the two states of the tunneling pair at some distance from the actual avoided crossing with the third state. Consequently both states have exponentially small weight in the barrier region, and we may expect a very strong localization. In Fig. 10 we can see that the asymmetric quantum breather at the degeneracy point δ
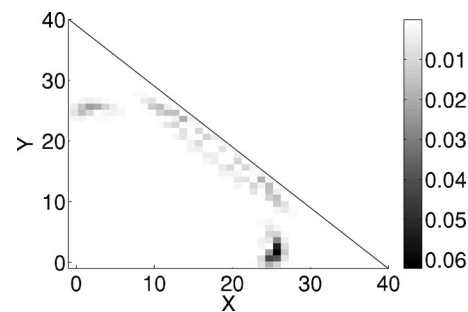

FIG. 7. Density of the asymmetric state $|\phi\rangle = (|\phi_{285}^{(S)}\rangle + |\phi_{268}^{(A)}\rangle)/\sqrt{2}$ as a function of the numbers of bosons at sites 1 and 2 at the degeneracy point δ_d. Here X is the number of bosons at site 1, and Y is the number of bosons at site 2.
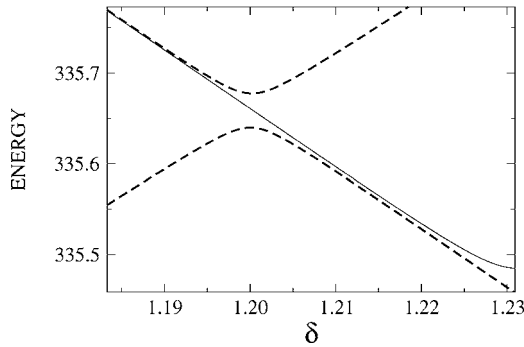
FIG. 8. An enlargement of the trimer spectrum around the avoided crossing 2 in Fig. 5, involving the symmetric state S-287 (thin solid line) and the antisymmetric states A-269 and A-270 (thick dashed lines).

FIG. 10. Density of the asymmetric state $|\phi\rangle=(|\phi_{284}^{(S)}\rangle +|\phi_{268}^{(A)}\rangle)/\sqrt{2}$ as a function of the number of bosons at sites 1 and 2 at the degeneracy point δ_d. Here X is the number of bosons at site 1, and Y is the number of bosons at site 2.

$\simeq 1.462$ in Fig. 9 (see arrow) is strongly localized and the tunneling is suppressed for all times. Note that in both cases two and three the order of the participating levels before and after the avoided crossing is not conserved, at variance to the first case we discussed above and which was described also in Ref. [40]. The above-mentioned strong localization of this exact asymmetric eigenstate is reflected in the fact that the wave function has practically zero weight around the barrier region $X=Y$ ($n_1=n_2$). Note that at variance with Fig. 7, here the wave function has no sizable contribution on the other side of the barrier. This state is thus very close to its classical discrete breather counterpart (Fig. 1). Indeed, for this state $\langle n_1\rangle=25.62$, $\langle n_2\rangle=2.38$, $\langle n_3\rangle=12.00$. Consequently we find a very strong localization for the expectation values, in addition to the observed asymmetry in Fig. 10.

It is interesting to test whether initial states with some distribution of bosons at every site of the trimer ($|\Psi_0\rangle =|n_0,m_0,l_0\rangle$) can significantly overlap with the above-described asymmetric eigenstates. This distribution is given

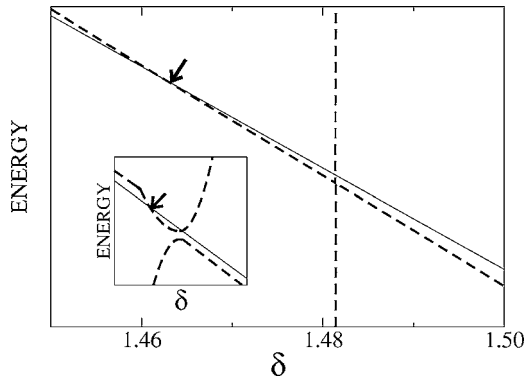by the maxima in the density for every asymmetric eigenstate (around $n_1=26$, and $n_2=2$). In Figs. 11 and 12 we show the time evolution of the expectation value of the number of bosons at every site on the trimer and the survival probability of such an initial excitation. A detailed analysis of the spectral intensity of the initial state $|\Psi_0\rangle=|26,2,12\rangle$ (inset in Fig. 12) shows that this initial excitation overlaps strongly with the degenerate eigenstates corresponding to the strong localization shown in Fig. 10. It implies that this excitation [Fig. 11(b)] will never distribute its quanta evenly over both sites of the dimer. For the case shown in Fig. 11(a) the initial excitation has a smaller overlap with the degenerate eigenstates, which gives the partial localization shown in Fig. 7. Since the overlap is not zero the excitation will also stay localized in the sense that the crossing of curves corresponding to $\langle n_1\rangle$ and $\langle n_2\rangle$ as in Figs. 3(a) and 3(b) will never occur. Note that despite the difference between the analyzed cases one and three, the evolutions of the expectation values and the survival probabilities do not differ drastically. It needs more sensitive details in the preparation of an initial state to

FIG. 9. An enlargement of the trimer spectrum around the avoided crossing 3 in Fig. 5, involving the symmetric state S-284 (thin solid line) and the antisymmetric states A-267 and A-268 (thick dashed lines). The curves for antisymmetric eigenstates were generated from the data $\Delta E(\delta)$ by using $E_A=E_S-\gamma\Delta E$, with $\gamma =1000$, for better visualization of intersection between eigenvalues. Inset: Sketch of the variation of eigenvalues participating in the avoided crossing. Thin solid line, symmetric eigenstate; thick dashed line, antisymmetric eigenstates. The arrows mark the analyzed degeneracy point (see text).
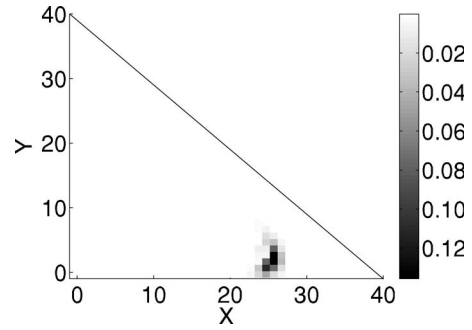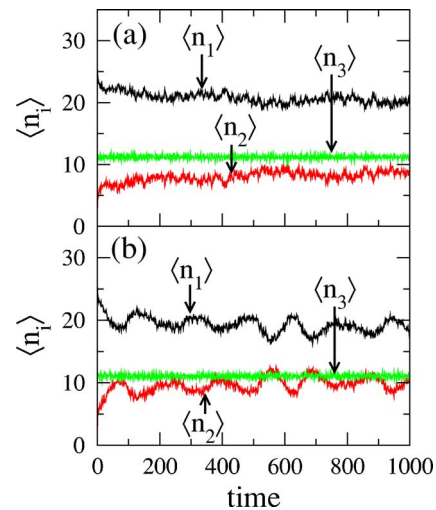

FIG. 11. (Color online) Time evolution of expectation values of the number of bosons at every site on the trimer at the degeneracy points for the cases shown in (a) Fig. 7, (b) Fig. 10. The initial state is $|\Psi_0\rangle=|26,2,12\rangle$.
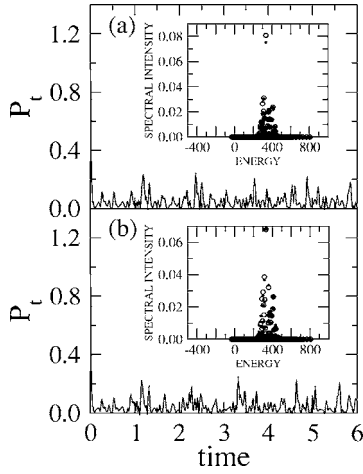
FIG. 12. Survival probability of the initial state $|\Psi_0\rangle$ $=|26,2,12\rangle$ at the degeneracy points for the cases shown in (a) Fig. 7, (b) Fig. 10. Inset: Spectral intensity of the initial state $|\Psi_0\rangle$. Filled circles, symmetric eigenstates; open circles, antisymmetric eigenstates.

observe a practically total localization of bosons on one of the dimer sites for case three as compared to case one.

IV. CONCLUSIONS

In this work we observed how spectral properties of the Hamiltonian are reflected in the time evolution of different localized excitations in a trimer molecule model by monitoring the spectrum, the time evolution of expectation values of the number of bosons at every site on the trimer, and survival probabilities of different localized excitations.

The tunneling pair splitting determines the lifetime of localized excitations. The survival probability and the time evolution of the expectation values of the number of bosons are clear indicators for a localized excitation being close to or far from a quantum breather tunneling pair, while the spectral intensity of localized excitations is typically broad and does not show the peculiarities of the tunneling dynamics. Probing the time evolution of initially localized excited states thus allows one to draw conclusions about the presence or absence of tunneling pair eigenstates.

We report on the existence of degenerate levels in the spectrum due to the presence of both avoided crossings and tunneling pairs. At these degenerate points tunneling is suppressed for all times. While in general the asymmetric exact eigenstates will have quite large weight in the dynamical barrier region (contributed by the single level), we observe specific parameter cases where the weight is very small and the corresponding asymmetric eigenstate very strongly localized. Full or partial localization of bosons appears for all time scales for some specific states and some specific values of the parameters. This effect could be studied in experimental situations of Bose-Einstein condensates in few traps which weakly interact, as well as in systems of few coupled Josephson junctions which operate in the quantum regime. Tuning experimental control parameters will allow one to lock localized excitations for specific values and both pre-

vent the excitation from tunneling, and allow for a fine tuning of the tunneling frequency from a small value down to zero in the vicinity of these specific control parameter values.

APPENDIX: EXPECTATION VALUES AND SURVIVAL PROBABILITY

Expanding the wave function in the basis of symmetric and antisymmetric eigenstates of the Hamiltonian

$$|\Psi_t\rangle = \sum_\mu \phi_0^{\mu(S)} e^{-iE_\mu^{(S)}t} |\phi^{\mu(S)}\rangle + \sum_\nu \phi_0^{\nu(A)} e^{-iE_\nu^{(A)}t} |\phi^{\nu(A)}\rangle, \tag{A1}$$

where $\phi_0^{\mu(S,A)} = \langle \phi^{\mu(S,A)} | \Psi_0 \rangle_{S,A}$ and $\phi_{n_1,n_2,n_3}^{\mu(S,A)} = \langle \phi^\mu | n_1, n_2, n_3 \rangle_{S,A}$, the expectation value of the number of bosons at site i is written as

$$\langle n_i \rangle(t) = \langle n_i^{(S)} \rangle(t) + \langle n_i^{(A)} \rangle(t) + \langle n_i^{(M)} \rangle(t), \tag{A2}$$

where

$$\langle n_1^{(S,A)} \rangle(t) = \frac{1}{4} \sum_{\mu,\mu'} \phi_0^{\mu(S,A)} \bar{\phi}_0^{\mu'(S,A)} e^{i(E_\mu^{(S,A)} - E_{\mu'}^{(S,A)})t} F_{\mu,\mu'}^{(S,A)}, \tag{A3}$$

$$\langle n_2^{(S,A)} \rangle(t) = \langle n_1^{(S,A)} \rangle(t), \tag{A4}$$

$$F_{\mu,\mu'}^{(S,A)} = \sum_{\{n_i\}_{S,A}} \bar{\phi}_{n_1,n_2,n_3}^{\mu(S,A)} (n_1 + n_2) \phi_{n_1,n_2,n_3}^{\mu'(S,A)}, \tag{A5}$$

$$\langle n_1^{(M)} \rangle(t) = \mathrm{Re}\left(\frac{1}{2} \sum_{\mu,\nu} \phi_0^{\mu(S)} \bar{\phi}_0^{\nu(A)} e^{i(E_\mu^{(S)} - E_\nu^{(A)})t} F_{\mu,\nu}^{(M)} \right), \tag{A6}$$

$$\langle n_2^{(M)} \rangle(t) = -\langle n_1^{(M)} \rangle(t), \tag{A7}$$

$$F_{\mu,\nu}^{(M)} = \sum_{\{n_i\}_A} \bar{\phi}_{n_1,n_2,n_3}^{\mu(S)} (n_1 - n_2) \phi_{n_1,n_2,n_3}^{\nu(A)}, \tag{A8}$$

$$\langle n_3^{(S,A)} \rangle(t) = \frac{1}{2} \sum_{\mu,\mu'} \phi_0^{\mu(S,A)} \bar{\phi}_0^{\mu'(S,A)} e^{i(E_\mu^{(S,A)} - E_{\mu'}^{(S,A)})t} G_{\mu,\mu'}^{(S,A)}, \tag{A9}$$

$$G_{\mu,\mu'}^{(S,A)} = \sum_{\{n_i\}_{S,A}} \bar{\phi}_{n_1,n_2,n_3}^{\mu(S,A)} (n_1 + n_2) \phi_{n_1,n_2,n_3}^{\mu'(S,A)}, \tag{A10}$$

$$\langle n_3^{(M)} \rangle(t) = 0, \tag{A11}$$

where overbars mean complex conjugation.

[1] T. Uzer, Phys. Rep. **199**, 73 (1991), and references therein.

[2] C. Jaffé and P. Brumer, J. Chem. Phys. **73**, 5646 (1980).

[3] S. Keshavamurthy, J. Chem. Phys. **122**, 114109 (2005);S. Keshavamurthy, Phys. Rev. E **72**, 045203 (2005).

[4] G. D. Carney, L. L. Sprandel, and C. W. Kern, Adv. Chem. Phys. **37**, 305 (1978); Z. Bačić and J. C. Light, Annu. Rev. Phys. Chem. **40**, 469 (1989), and references therein.

[5] Comput. Phys. Commun. **51** (1) and (2) (1988), thematic issue on molecular vibrations, edited by J. M. Bowman.

[6] M. Joyeux, S. Yu. Grebenshchikov, J. Bredenbeck, R. Schinke, and S. C. Farantos, Adv. Chem. Phys. **130**, 267 (2005).

[7] J. C. Eilbeck, P. S. Lomdahl, and A. C. Scott, Physica D **16**, 318 (1985).

[8] S. Flach and C. R. Willis, Phys. Rep. **295**, 181 (1998).

[9] D. K. Campbell, S. Flach, and Y. S. Kivshar, Phys. Today **57**(1), 43, (2004).

[10] A. J. Sievers and J. B. Page, in *Dynamical Properties of Solids VII: Phonon Physics. The Cutting Edge*, edited by G. K. Horton and A. A. Maradudin (Elsevier, Amsterdam, 1995), p. 137.

[11] S. Aubry, Physica D **103**, 201 (1997).

[12] U. T. Schwarz, L. Q. English, and A. J. Sievers, Phys. Rev. Lett. **83**, 223 (1999).

[13] M. Sato and A. J. Sievers, Nature (London) **432**, 486 (2004).

[14] B. I. Swanson, J. A. Brozik, S. P. Love, G. F. Strouse, A. P. Shreve, A. R. Bishop, W.-Z. Wang, and M. I. Salkola, Phys. Rev. Lett. **82**, 3288 (1999).

[15] E. Trias, J. J. Mazo, and T. P. Orlando, Phys. Rev. Lett. **84**, 741 (2000).

[16] P. Binder, D. Abraimov, A. V. Ustinov, S. Flach, and Y. Zolotaryuk, Phys. Rev. Lett. **84**, 745 (2000).

[17] H. S. Eisenberg, Y. Silberberg, R. Morandotti, A. R. Boyd, and J. S. Aitchison, Phys. Rev. Lett. **81**, 3383 (1998).

[18] J. W. Fleischer, M. Segev, N. K. Efremidis, and D. N. Christodoulides, Nature (London) **422**, 147 (2003).

[19] M. Sato, B. E. Hubbard, A. J. Sievers, B. Ilic, D. A. Czaplewski, and H. G. Craighead, Phys. Rev. Lett. **90**, 044102 (2003).

[20] A. Trombettoni and A. Smerzi, Phys. Rev. Lett. **86**, 2353 (2001).

[21] E. A. Ostrovskaya and Y. S. Kivshar, Phys. Rev. Lett. **90**, 160407 (2003).

[22] B. Eiermann, Th. Anker, M. Albiez, M. Taglieber, P. Treutlein, K.-P. Marzlin, and M. K. Oberthaler, Phys. Rev. Lett. **92**, 230401 (2004).

[23] A. Smerzi, S. Fantoni, S. Giovanazzi, and S. R. Shenoy, Phys. Rev. Lett. **79**, 4950 (1997).

[24] S. Raghavan, A. Smerzi, S. Fantoni, and S. R. Shenoy, Phys. Rev. A **59**, 620 (1999).

[25] M. Albiez, R. Gati, J. Fölling, S. Hunsmann, M. Cristiani, and M. K. Oberthaler, Phys. Rev. Lett. **95**, 010402 (2005).

[26] A. C. Scott and J. C. Eilbeck, Phys. Lett. A **119**, 30 (1986).

[27] L. J. Bernstein, Physica D **68**, 174 (1993).

[28] S. Aubry, S. Flach, K. Kladko, and E. Olbrich, Phys. Rev. Lett. **76**, 1607 (1996).

[29] L. Bernstein, J. C. Eilbeck, and A. C. Scott, Nonlinearity **3**, 293 (1990).

[30] G. Kalosakas and A. R. Bishop, Phys. Rev. A **65**, 043616 (2002).

[31] G. Kalosakas, A. R. Bishop, and V. M. Kenkre, J. Phys. B **36**, 3233 (2003).

[32] D. A. Garanin, J. Phys. A **24**, L61 (1991).

[33] D. A. Garanin, E. M. Chudnovsky, and R. Schilling, Phys. Rev. B **61**, 12204 (2000).

[34] M. Davis and E. Heller, J. Chem. Phys. **75**, 246 (1981).

[35] E. Wright, J. C. Eilbeck, M. H. Hays, P. D. Miller, and A. C. Scott, Physica D **69**, 18 (1993).

[36] S. Flach and V. Fleurov, J. Phys.: Condens. Matter **9**, 7039 (1997).

[37] S. De Fillippo, M. Fusco Girard, and M. Salerno, Nonlinearity **2**, 477 (1989).

[38] A. Chefles, J. Phys. A **29**, 4515 (1996).

[39] L. Cruzeiro-Hansson, H. Feddersen, R. Flesch, P. L. Christiansen, M. Salerno, and A. C. Scott, Phys. Rev. B **42**, 522 (1990).

[40] S. Flach, V. Fleurov, and A. A. Ovchinnikov, Phys. Rev. B **63**, 094304 (2001).

[41] R. T. Lawton and M. S. Child, Mol. Phys. **40**, 773 (1980).

[42] M. S. Child and R. T. Lawton, Faraday Discuss. Chem. Soc. **71**, 273 (1981).

[43] E. L. Sibert III, W. P. Reinhardt, and J. T. Hynes, J. Chem. Phys. **77**, 3595 (1982).

[44] G. M. Schmidt, S. L. Coy, R. W. Field, and R. J. Silbey, J. Chem. Phys. **101**, 869 (1994).

[45] M. E. Kellman, Annu. Rev. Phys. Chem. **46**, 395 (1995), and references therein.